Multiple Ion Association versus Redissociation in Aqueous NaCl and KCl at High Temperatures

Andrei V. Sharygin,[§] Robert H. Wood, Gregory H. Zimmerman,[||] and Victor N. Balashov*,[‡]

Department of Chemistry and Biochemistry, University of Delaware, Newark, Delaware 19716

Received: September 27, 2001; In Final Form: March 29, 2002

The electrical conductivities of aqueous solutions of NaCl have been measured at 651 and 670 K at 28 MPa for molalities up to 1.0 mol kg^{-1}. These conductivities as well as the results of Hwang et al. (*High Temp. High Pres.* **1970**, *2*, 651−669), Ritzert and Franck (*Ber. Bunsen-Ges. Phys. Chem.* **1968**, *72*, 798−808), and Mangold and Franck (*Ber. Bunsen-Ges. Phys. Chem.* **1969**, *73*, 21−27) for aqueous KCl have been fit to the conductance equation of Turq et al. (*J. Phys.Chem.* **1995**, *99*, 822−827) with a consensus mixing rule and either mean spherical approximation or Debye−Hückel activity coefficients. Except at one state point (NaCl at 670 K and 28 MPa), where the interactions are the strongest ($\beta^* = 17.8$), the simplest model that fits the experimental results reasonably well (± 2−3%) at molalities up to 4.5 mol kg^{-1} is one with only the limiting equivalent conductance and a pair association constant adjusted. Activity coefficients calculated with either the MSA and ionic diameters or with the Debye−Hückel equation of Oelkers and Helgeson (*Geochim. Cosmochim. Acta* **1990**, *54*, 727−738) (with no salting out) can be used with similar accuracy. At high concentrations this model predicts strong redissociation of the ion pairs that form at low concentrations. Oelkers and Helgeson (*Geochim. Cosmochim. Acta* **1993a**, *57*, 2673−2697) proposed a model with substantial multi-ion association (triplets and quartets, etc.). This model has two more adjustable parameters and does not fit the data without the physically unrealistic salting out coefficient used by Oelkers and Helgeson (*Geochim. Cosmochim. Acta* **1991**, *55*, 1235−1251), so this model is not recommended. For the point with the highest β^*, more complex models are needed at concentrations above 0.05 mol kg^{-1}. Good fits to the data were found for multi-ion association models (five adjustable parameters) and reasonable fits for more complex activity models (four adjustable parameters) with only pair association, so that the models are about equally accurate at equal complexity. The cluster model of Laria et al. (*J. Chem. Soc., Faraday Trans.* **1990**, *86*, 1051−1056) for the restricted primitive model is consistent with the qualitative predictions of our preferred model with only pair association.

1. Introduction

A knowledge of the activity coefficients and association constants of alkali halides, in particular NaCl (aq) and KCl (aq), are important in a variety of geochemical and industrial processes. In particular this knowledge is necessary for the prediction of mineral alteration, solubility, transport, and deposition by hydrothermal brines.[1−3] Industrially, these reactions are important in understanding corrosion in electric and hydrothermal power plants. In hydrothermal solutions the ion pairing of many alkali halides has been measured using electrical conductance starting with the pioneering work of Noyes et al.[4] and continued by Fogo et al.,[5] Franck et al.,[6,7] Marshall et al.,[8,9] and many others. At high temperatures the equivalent conductance drops with increasing concentration then levels off or even rises before dropping again. This same behavior is well known in many other low dielectric constant solvents.[10] At low molalities (below about 0.01 mol kg^{-1} in water), conductance equations and activity models explain the drop in conductance and allow the determination of the limiting equivalent conductance and the pairwise association constant with excellent accuracy. Hwang et al.[11] found on the basis of the high temperature and pressure experimental data for LiCl, LiBr, and CsCl at high molalities $m > 7$ mol kg^{-1}, that the transport properties of these aqueous concentrated electrolyte solutions could be better explained by starting from the properties of electrolyte melts, rather than by extrapolation from the region of dilute solutions. Thus, they postulated redissociation of the ion pairs present in dilute solutions. At these high molalities, Valyashko[12] showed that the solutions of aqueous halides behaved as solvated molten salts. In an alternate explanation, Oelkers and Helgeson[2] proposed that multi-ion aggregates become increasingly important from intermediate up to high concentrations until eventually a single giant aggregate is present, i.e., a solvated molten salt. They used a salting out coefficient determined from conductance data with provisional estimates of association constants for three-, four-, five-, and six-ion aggregates to calculate speciation in a variety of high temperature NaCl (aq) solutions. These predictions of association constants are the only ones available.

In a discussion, Eric Oelkers suggested to one of us (R.H.W.) that a multi-ion association rather than a large salting out

* Corresponding author. Present address: University of Delaware.
‡ Institute of Experimental Mineralogy, Chernogolovka, Moscow District 142432.
§ Present address: Congoleum Corporation, Research and Development, P.O. Box 3127, 861 Sloan Avenue, Mercerville, NJ 08619.
|| Present address: Bloomsburg University, Chemistry Department, Bloomsburg, PA 17815-1301.

10.1021/jp013647u CCC: $22.00
Published on Web 06/13/2002

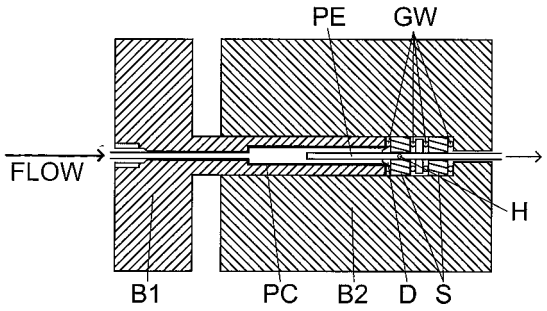

Figure 1. Cross section of the new conductance cell. B1 and B2 are cylindrical steel blocks; PC is the platinum cup; D is the diamond shield; S are the saphire insulators; H is a hole for the solution exit; GW are the gold or graphite washers; and PE is the platinum electrode.

coefficient might explain the conductance measurements that led to the use of a high salting out coefficient. The present research was motivated by the suggestion of Oelkers plus the recent development in our laboratory of (1) a high-temperature conductance apparatus capable of increased precision; (2) the development by Turq and co-workers[13,14] of a conductance equation that can fit data at higher concentrations (TBBK equation); and (3) a consensus model for the conductance of mixtures given the conductance of a single electrolyte.[15,16]

From a rigorous statistical mechanical point of view, either model with an accurate theory would be equally valid, and the amount of ion aggregation would depend on the arbitrary definitions of ion-pairs and multi-ion aggregates. The goal of the present investigation was to find the simplest model (with fewest adjustable parameters) that would fit the data.

In this paper we present new high concentration experimental results for NaCl (aq) at two state points together with fits of various models to these data and to measurements from the literature on KCl (aq).[6,711] We found that the simplest model that reproduces most of the experimental data is a model with only pairwise association and ion activities calculated with either the mean spherical approximation (MSA) or an extended Debye−Hückel equation (DH). When the dielectric constant is very low a complex model is needed to fit the data, and either redissociation or multi-ion aggregates can fit the data.

2. Experimental Section

A new conductance apparatus was designed to measure the conductivity of aqueous solutions at high temperatures and pressures using a flow-through method developed in this laboratory.[17,18] This apparatus has the advantage that the pressure on the sapphire insulators is more uniform so cracking is no longer a serious problem.

The conductance cell (see Figure 1) was contained within a steel block, B1 and B2. B2 was 75.6 mm in diameter and 88.2 mm long. The outer electrode of the conductance cell (PC) was formed from a platinum/rhodium cylinder (5.6 mm o.d., 4.6 mm i.d., 39 mm length, 80% Pt-20% Rh by mass; Engelhard, Inc.) gold-soldered to a platinum/rhodium disk (5.6 mm o.d., 1.0 mm i.d., 0.5 mm thickness) to form a cup into which the solution flowed. The inlet tubing was gold-soldered into a hole in the disk. The inner electrode (PE) was made from a piece of Pt/Rh tubing (1.6 mm o.d., 1.0 mm i.d.), gold filled at one end, that was passed through the center of a cylindrical sapphire insulator (S) (12.7 mm o.d., 1.8 mm i.d., 6.4 mm length, Insaco, Inc.) and inserted 3.2 cm into the outer electrode. A CVD diamond washer (D) (4.4 mm o.d., 1.7 mm i.d., 1 mm thickness; Harris Diamond Corp.) was used to shield the surface of the sapphire where it had a contact with measured solutions. This allows measuring acids and bases, which do not attack the diamond shield. A platinum−rhodium washer (9.5 mm o.d., 1.6 mm i.d., 1 mm thickness) was gold-soldered around the base of the inner electrode and served as a compression plate to seal the conductance cell. Two gold washers (GW) were placed on both sides of the first sapphire insulator. Two additional graphite washers (GW) were placed on both sides of the second sapphire insulator. The graphite washers were fabricated from 0.4 mm thickness graphite tape (Union Carbide Corp.). A small hole (H) was drilled in the inner electrode just before the compression plate to allow the solution to flow out of the conductance cell. The hole also swept any dissolving sapphire away from the conductance cell. Solutions exited the cell via Pt/Rh capillary tubing (1.0 mm o.d., 0.5 mm i.d.) that was gold-soldered into the inner electrode after the compression plate.

The conductance block was suspended between two semicylindrical (229 mm length, 153 mm o.d., 107 mm i.d.) ceramic plates. These plates provided a layer of insulation around the conductance block. The block assembly was surrounded by two open aluminum boxes (one top and one bottom, measuring 360 mm length, 280 mm width, 140 mm height) that were sealed to form the primary heater box for the conductance cell. An additional aluminum box, formed from two open aluminum boxes (1050 mm length, 400 mm width, bottom box 210 mm height, top box 270 mm height) surrounded the inner box and was packed with Fiberfrax Durablanket ceramic fiber insulation (Carborundum Corp.). The outside of the aluminum box was packed with 65 mm of additional Fiberfrax insulation. The aluminum boxes were used to reduce the convection currents and thereby temperature gradients through the high-temperature zone. To further reduce temperature gradients caused by convection currents, glass strips were placed on top of the Fiberfrax insulation between the top half of the box and the bottom half.

The principal heat for the conductance apparatus was supplied by 4×125 W strip heaters. The heaters were wired in parallel configuration using a 16-gauge stainless steel rod bent to the correct shape and length and spot-welded to the strip-heater lead posts. These heaters were bolted to a 5 mm thick stainless steel plate fastened to the bottom of the inner aluminum box. Temperature was controlled by a 100 Ω RTD embedded with ceramic cement in a 3 mm groove in the stainless steel plate. The RTD formed one arm of a Wheatstone bridge circuit across which an Electromax III Leeds and Northrup temperature controller was used to control the heater power. Additional temperature control was supplied to the cell by two 135 W each, 120 V cartridge heaters inserted in a predrilled hole in the conductance block. These heaters were used to fine-tune the temperature of the conductance block to the desired experimental temperature and were controlled by a 1000 Ω RTD and an Electromax III temperature controller.

A coaxial resistance heater (515 mm length, 3 mm o.d.) was used to heat the inlet stream to the desired temperature. The heater was silver soldered to a stainless steel tube (1.6 mm o.d., 1.2 mm i.d.) that fit snugly around the platinum/rhodium inlet tube. The air gap between the two tubes was estimated to be no more than 0.03 mm. A thermocouple between the conductance block and the inlet tube was connected to an Electromax III temperature controller and adjusted the inlet flow temperature to the temperature of the conductance cell. The thermocouple was attached to the inlet tube approximately 2 cm from the conductance block using ceramic cement. Care was taken to ensure no electrical contact was made between the thermocouple and the inlet tube. A layer of ceramic cement was placed on

the inlet tube and allowed to dry before the thermocouple was fastened with additional ceramic cement to the initial layer. The other end of the thermocouple was attached to the conductance block in a similar manner, with the exception that the thermocouple contact was inserted into a ceramic capillary tube that fit snugly into a hole in the conductance block. This assembly was then secured with ceramic cement. At high temperatures several experiments were made with two different flow rates to ensure that the thermal equilibration was complete. These experiments showed that the solutions, flowing into the cell, were well equilibrated with the block, since the difference in measured conductivity at different flow rates was within the experimental uncertainties. The temperature gradient between the inflow tubing and the conductance block was also periodically measured with an iron−constantan thermocouple. The voltage across the thermocouple was never greater than 5 mV corresponding in temperature to about 0.1 K.

Resistances were measured at frequencies of 1 kHz and 10 kHz using an RCL meter (Fluke Co.; model PM6304c) with manufacturer's stated accuracy of 0.05% at 1 kHz and 0.1% at 10 kHz. All measured resistances were corrected for the lead resistance and linearly extrapolated to infinite frequency as a function of the inverse of the square root of the frequency. Lead resistances were always less than 0.5% of the solutions resistance. The temperature was measured with a platinum resistance standard (Hart Scientific; model 5612) with a stated calibration accuracy of ±0.007 K at 273 K, ±0.024 K at 473 K, and ±0.033 K at 673 K. The solution was introduced inside of the conductance apparatus using an HPLC pump (Waters, Division of Millipore, Inc.; model 590), which was operated at a constant flow rate of 8.3×10^{-3} cm^3 s^{-1}. The pressure was measured using a Digiquartz pressure transducer (ParoScientific, Inc.; model 760-6K) with an accuracy of ±0.01 MPa. The temperature and pressure were recorded immediately after a stable reading of resistance was achieved, corresponding to a sample plateau.

The cell constant was first determined before all reported measurements by a series of four measurements on dilute aqueous solutions of KCl (with molarities from 10^{-4} to 10^{-2} mol dm^{-3}) at $T = 298.15$ K and $p = 25.3$ MPa. The cell constant was calculated using the results of Fisher and Fox[19] at these conditions. Calculated cell constants agreed within 0.1% over the complete range of concentrations. The cell constant was also determined at $T = 298.15$ K and $p = 0.4$ MPa after all measurements were completed. The calculations at these conditions were done using equations given by Justice[20] for KCl (aq). The cell constant was found to be lower by 0.8% than the initial value. Similar changes in the cell constant were reported previously by Zimmerman et al.[17] and Gruszkiewicz and Wood.[18] These changes are caused by small changes of the cell dimensions with time due to annealing at high temperatures. It was concluded previously[18] that, although the changes in the cell constant influence directly the conductance results, the calculated equilibrium constants are not significantly affected. The average value of the cell constant at 298 K, $h = (0.0528 \pm 0.0002)$ cm^{-1} was used in all calculations. The cell constant at elevated temperatures was calculated from the known thermal expansion of the platinum cup, inner electrode, and sapphire insulator.

The solutions of KCl used in the calibration of the cell were prepared by mass from certified A. C. S. grade KCl (Fisher Scientific Co.; maximum impurity was mass fraction 10^{-4} of Br$^-$) and distilled and deionized water. The salt was dried for 24 h at $T = 573$ K, cooled in a desiccator under vacuum, and diluted by mass with conductivity water to the initial molality. All apparent masses were corrected for buoyancy.

TABLE 1: Equivalent Conductance (Λ/S cm^2 equiv^{-1}) of Aqueous NaCl at Temperature (T/K), Pressure (P/MPa), Molality (m/mol/kg), Concentration (c/mol/dm^3), and Specific Conductivity of Water (κ_s/S cm^{-1})

T/K	P/MPa	ρ^{0a}	$m\ 10^3$	$c\ 10^3$	Λ	$\kappa_s\ 10^6$
651.25	27.96	524.30	0.0445	0.0234	1221.1	0.881
651.24	27.95	524.25	0.1840	0.0965	1205.9	0.881
651.24	27.92	524.87	0.6769	0.3549	1148.9	0.881
651.24	27.92	523.91	4.663	2.449	961.8	0.881
651.21	27.92	524.10	17.35	9.1547	775.95	0.881
651.22	27.93	524.14	44.61	23.75	646.19	0.881
651.30	27.92	524.53	101.5	54.83	551.52	0.881
651.27	27.95	524.04	253.6	141.5	490.77	0.881
651.38	27.99	523.85	444.7	255.4	482.36	0.881
651.38	27.99	523.80	704.4	420.0	501.99	0.881
651.35	28.01	524.24	1027.3	627.0	372.23	0.881
670.16	28.00	298.26	0.0031	0.00091	1269.3	0.120
670.14	28.00	298.57	0.0083	0.0025	1257.2	0.120
670.11	28.00	299.04	0.0317	0.0095	1184.9	0.120
670.07	28.00	299.67	0.138	0.0412	968.99	0.120
670.05	28.00	299.98	0.522	0.157	701.70	0.120
670.04	28.00	300.14	4.350	1.319	356.74	0.120
670.04	28.00	300.14	15.71	4.837	235.57	0.120
670.15	28.01	299.03	0.0389	0.0116	1179.8	0.144
670.20	28.03	299.52	0.136	0.041	968.40	0.144
670.19	28.03	299.61	0.578	0.174	672.51	0.144
670.17	28.00	298.08	4.356	1.310	343.46	0.144
670.23	28.04	299.54	17.09	5.271	227.99	0.144
670.25	28.04	299.23	45.81	14.74	185.62	0.144
670.22	27.98	296.09	101.5	34.82	173.89	0.144
670.15	27.96	296.03	253.6	100.9	210.65	0.144
670.35	27.99	294.83	444.7	198.3	254.89	0.144
670.29	28.01	296.87	704.4	345.5	305.15	0.144
670.22	27.98	296.21	1027.3	541.7	293.51	0.144

[a] The density of pure water at T and P (kg/m3).

Stock solutions of sodium chloride were prepared by mass from A. C. S. grade NaCl (Fisher Scientific Co.; largest impurity, mass fraction 10^{-4} of Br$^-$) and conductivity water.

The salt was dried overnight at $T = 673$ K, cooled under vacuum, and diluted with conductivity water. To check that the solutions had not changed during the course of the measurement (±0.1%), the conductances of all stock solutions were measured at room temperature immediately after all experiments were completed. The conductivity water used in all measurements and preparations of stock solutions was first treated using a reverse osmosis system, then passed through one carbon adsorbent and two deionization tanks (Hydro Service and Supplies, Inc.; Picosystem, model 18). The resulting specific conductance of water was about 2×10^{-5} S m^{-1} at $T = 298$ K. The solvent conductance was measured at each temperature and pressure. The present results at $T = 298$ K are in good agreement with the literature data for NaCl.

The experimental equivalent conductance of NaCl (aq), Λ, corrected for impurities and specific conductivity of solvent (water), κ_s, at each temperature and pressure are listed in Table 1. The molar concentrations that are listed in Table 1 were calculated from molalities using the solvent densities taken from the Hill equation of state for H_2O.[21] The differences between the densities of pure solvent and those of solutions were calculated using the experimental densities of NaCl (aq) obtained at $T = 298$ K from Millero et al.[22] and at $T = (651$ to $670)$ K from Majer et al.[23]

The KCl conductance data in the range of 0.12−4.53 mol kg^{-1} and the relative densities of KCl solutions with the reference point of 298.15 K and 0.1 MPa were taken from Hwang et al.[11] To convert the relative density data to absolute values we used the density data at 298.15 K for KCl aqueous solutions reported by Vaslow.[24] The KCl conductance data of Ritzert and Franck[6] and Mangold and Franck[7] in the range of

TABLE 2: Equivalent Conductance of KCl Solutions

P MPa	$\rho^0(H_2O)$	*m*	*c*	Λ
T = 473.15 K				
20	878.03	0.001	0.00088	774.3
		0.002	0.00176	722.2
		0.010	0.00880	666.0
		0.11874	0.10349	587
		0.23826	0.20721	548
		0.50299	0.43516	482
		1.0211	0.87230	467
		2.1080	1.7584	437
		4.5266	3.5446	378
100	923.718	0.001	0.00093	744.3
		0.002	0.00185	679.6
		0.01	0.00926	643.1
		0.11874	0.10891	560
		0.23826	0.21759	528
		0.50299	0.45642	466
		1.0211	0.91186	438
		2.1080	1.8277	415
		4.5266	3.687	357
200	966.465	0.001	0.00097	716.3
		0.002	0.00194	648.5
		0.01	0.00969	621.8
		0.11874	0.11363	534
		0.23826	0.22680	500
		0.50299	0.47373	447
		1.0211	0.94647	400
		2.1080	1.9068	367
		4.5266	3.7978	333
300	1000.95	0.001	0.001	691.4
		0.002	0.002	624.3
		0.01	0.01	604.5
		0.11874	0.11765	508
		0.23826	0.23458	474
		0.50299	0.49005	427
		1.0211	0.97614	387
		2.1080	1.9721	355
		4.5266	3.9164	314
T = 573.15 K				
100	823.108	0.001	0.00083	958.6
		0.002	0.00165	857.3
		0.010	0.00825	823.8
		0.11874	0.09747	719
		0.23826	0.19541	674
		0.50299	0.41142	579
		1.0211	0.82680	556
		2.1080	1.6793	498
		4.5266	3.4219	421
200	885.202	0.001	0.00089	896.0
		0.002	0.00178	802.3
		0.01	0.00887	782.5
		0.01[b]	0.00887	788.7
		0.11874	0.10419	679
		0.23826	0.20886	638
		0.50299	0.43912	554
		1.0211	0.87922	495
		2.1080	1.7743	438
		4.5266	3.5881	382
300	930.016	0.001	0.00093	844.7
		0.002	0.00187	762.8
		0.01	0.00932	741.0
		0.01[b]	0.00932	748.9
		0.11874	0.10939	643
		0.23826	0.21901	605
		0.50299	0.45939	532
		1.0211	0.91779	472
		2.1080	1.8573	421
		4.5266	3.7186	368
T = 673.15 K				
100	692.857	0.001	0.00069	1114.6
		0.002	0.00139	1016.8
		0.010	0.006946	955.0
		0.010[b]	0.006946	954.6
		0.11874	0.08225	749
		0.23826	0.16662	689
		0.50299	0.35307	583
		1.0211	0.71900	535
		2.1080	1.4875	492
		4.5266	3.1173	423
200	792.24	0.001	0.00079	1043.5
		0.002	0.00159	955.7
		0.01	0.00794	891.7
		0.01[b]	0.00794	888.9
		0.11874	0.09346	737
		0.23826	0.18786	695
		0.50299	0.3956	594
		1.0211	0.79911	519
		2.1080	1.6279	456
		4.5266	3.3507	394
300	852.496	0.001	0.00085	992.7
		0.002	0.00171	911.1
		0.01	0.00855	840.0
		0.01[b]	0.00855	844.2
		0.11874	0.10042	708
		0.23826	0.20131	673
		0.50299	0.42329	579
		1.0211	0.85252	505
		2.1080	1.7288	446
		4.5266	3.5248	377
T = 773.15 K				
100	528.427	0.001	0.00053	1077.5
		0.002	0.00106	951.8
		0.010	0.00530	848.3
		0.11874	0.06325	608
		0.23826	0.10880	556
		0.50299	0.27692	496
		1.0211	0.57461	463
		2.1080	1.2303	450
		4.5266	2.7217	407
200	691.207	0.001	0.00069	1089.3
		0.002	0.00139	990.2
		0.01	0.00693	920.1
		0.01[b]	0.00693	910.6
		0.11874	0.08189	731
		0.23826	0.15316	689
		0.50299	0.34926	590
		1.0211	0.71208	518
		2.1080	1.4677	465
		4.5266	3.0778	410
300	771.383	0.001	0.00077	1038.8
		0.002	0.00155	950.2
		0.01	0.00773	889.0
		0.01[b]	0.00773	884.8
		0.11874	0.09098	733
		0.23826	0.17417	696
		0.50299	0.38532	585
		1.0211	0.78329	528
		2.1080	1.5923	465
		4.5266	3.2993	395
T = 873.15 K				
200	589.939	0.001	0.00059	1045.9
		0.002	0.00118	950.3
		0.01	0.00591	840.9
		0.11874	0.06974	598
		0.23826	0.14136	578
		0.50299	0.30066	478
		1.0211	0.62505	441
		2.1080	1.3055	429
		4.5266	2.7534	375
300	691.051	0.001	0.00069	1043.6
		0.002	0.00139	960.3
		0.01	0.00693	890.2
		0.01[b]	0.00693	882.6
		0.11874	0.08166	675
		0.23826	0.16496	660
		0.50299	0.34912	548
		1.0211	0.71208	495
		2.1080	1.4697	460
		4.5266	2.9987	384

[a] The symbols and units are the same as in Table 1. The first three entries are interpolated from Ritzert and Franck.[6] The data for molalities above 0.1 mol/kg are from Hwang et al.[11] [b] The interpolated value from the Mangold and Franck[7] data.

0.001−0.01 mol kg^{-1} was interpolated with second-order accuracy to the same temperatures and densities as in Hwang et al.[11] The results are listed in Table 2. The reported accuracy of the KCl conductance results is about 2 to 3%.

3. Theory

3.1. Fitting Conductance Data. Our equation for the conductance of a reacting mixture of electrolytes has three

components: (1) a model for the activity coefficients of the ions so that the equilibrium concentrations of free ions in a reacting mixture can be calculated from the equilibrium constants for the reactions; (2) an equation for the equivalent conductivity of a single strong electrolyte as a function of concentration; (3) a mixing rule that predicts the conductance of a mixture of strong electrolytes from the conductance of the single electrolytes. Recently, Sharygin et al.[16] have tested this model and have shown that it allows the calculation of association constants from conductance measurements of solutions containing a mixture of ions. Sharygin et al.[16] give complete details of the equations used in our model. Below we will discuss briefly the model and a few additions that are necessary in applying the model at high concentrations.

3.2. Multiple Ion Association. In general, for a 1:1 electrolyte solution AB, A = cation and B = anion, we assume the existence of $A_{\nu_1}B_{\nu_2}^{\nu_1-\nu_2}$ ion aggregates with charge $(\nu_2 - \nu_1)$. We characterize the ion equilibria in solution by overall dissociation reactions:

$$A_{\nu_1}B_{\nu_2}^{\nu_1-\nu_2} = \nu_1 A^+ + \nu_2 B^- \tag{1}$$

The thermodynamic expression of mass action law of eq 1 has the form

$$K_{\mathrm{ci}} = \frac{a_{A^+}^{\nu_1} a_{B^-}^{\nu_2}}{a_{A_{\nu_1}B_{\nu_2}^{\nu_1-\nu_2}}} \tag{2}$$

where K_{ci} is the overall dissociation constant of an ion cluster in the molal concentration scale with cluster index $ci = \nu_1 + \nu_2$, and a_α are the molal activities of species in solution. We assume that the value of thermodynamic dissociation constant is defined by cluster index *ci*. Thus the dissociation constants of A_2B^+ and AB_2^- are assumed to be the same: $K[A_2B^+] = K[AB_2^-] = K_3$. This assumption is probably not bad because of the electrostatic nature of ion clusters.[1] It should be noted that clusters with $|\nu_1 - \nu_2| > 1$ are neglected because of their high charge.

3.3. Activity Coefficient Models. We have used two different models for the activity coefficients: the mean spherical approximation (MSA) and an extended Debye−Hückel limiting law. The MSA equation is much more accurate than the Debye−Hückel equation for the activity coefficients of hard spheres in a continuous dielectric medium, and it is still an analytic equation. It is more accurate because it conforms to both the Debye−Hückel limiting law at low concentrations and the hard sphere repulsion limiting law in very concentrated solutions. Both equations apply to a hard sphere ion in a continuous dielectric medium, and both equations are rigorously applicable only to the MacMillan−Mayer standard state.[25] In our calculations we ignored the corrections to the MacMillan−Mayer standard state. Also as needed, we added second osmotic virial coefficients to the equations to correct for the fact that the short-range interactions in an aqueous solution are not the same as those for hard spheres in a continuous dielectric medium.

The activity coefficient at $c = 1$ mol dm^{-3} standard state in the MSA approximation can be expressed in the form of electrostatic (el) and hard sphere (hs) contributions:

$$\ln y_i^{\mathrm{MSA}} = \ln y_i^{\mathrm{el}} + \ln y_i^{\mathrm{hs}} \tag{3}$$

The MSA expression[26] for the electrostatic part is

$$\ln y_i^{\mathrm{el}} = -\frac{e^2}{4\pi\epsilon_0\epsilon k_{\mathrm{B}}T}\left(\frac{\Gamma z_i^{\,2}}{1+\Gamma\sigma_i} + \frac{\pi}{2}\left(\frac{P_n}{\Delta}\right)^2 \left(\sum_j \rho_j\right)^{-1}\right) \tag{4}$$

where e is the electronic charge, k_{B} is Boltzmann's constant, ϵ_0 and ϵ are the dielectric constants of vacuum and solvent, respectively, σ_i is the diameter of ion i and ρ_i is the concentration of ion i. The shielding parameter Γ calculated as the solution to

$$4\Gamma^2 = \frac{e^2}{\epsilon_0\epsilon k_{\mathrm{B}}T}\sum_i \rho_i \left(\frac{z_i - \frac{\pi}{2\Delta}P_n\sigma_i^{\,2}}{1+\Gamma\sigma_i}\right)^2 \tag{5}$$

with

$$P_n = \left(1 + \frac{\pi}{2\Delta}\sum_k \frac{\rho_k\sigma_k^{\,3}}{1+\Gamma\sigma_k}\right)^{-1} \sum_k \frac{\rho_k\sigma_k z_k}{1+\Gamma\sigma_k}$$

$$\Delta = 1 - \frac{\pi}{6}\sum_k \rho_k\sigma_k^{\,3} \tag{6}$$

These equations can be greatly simplified by assuming a constant average diameter for all the ions with a different average for the electrostatic and the hard sphere radii.[27] We used the full equations because there were occasionally significant differences in the AAD of the fits (up to 1.5%) and the fits with the full equations were normally better. Thus, we found no real advantage in using the truncated equation. Following Turq et al.,[14] we neglected the terms P_n in eq 4 but not in eq 5, where this parameter is important for finding an accurate value of Γ.

The first and simplest choice for the hard sphere diameters of the ions is to use the crystallographic diameters in the equations so that there are no adjustable parameters. The radii of ion clusters were calculated from the expression

$$r_{\mathrm{ic}} = \sqrt[3]{\nu_1 r_{A^+}^{\,3} + \nu_2 r_{B^-}^{\,3}} \tag{7}$$

where r_{A^+} and r_{B^-} are the crystallographic radii of cation and anion. We tried two methods to adjust the equation for the fact that the short-range forces between the ions were not those between hard spheres in a continuous dielectric. If an adjustment is necessary, the easiest thing to do is scale all of the diameters by a uniform scaling factor (HSC). The second method is to add adjustable second osmotic virial coefficients for the interactions between pairs of species. These pairwise interaction coefficients adjust the interactions for the inadequacies of the MSA model in real solutions. To do this we add a term $\ln y_i'$ to the MSA equation where

$$\ln y_i' = 2.303 \sum_j b_{ij} c_j \tag{8}$$

In this equation it is necessary for thermodynamic consistency to have $b_{ij} = b_{ji}$. This is because, for instance, if an ion salts out a pair then the pair must salt out the ion with exactly the same interaction coefficient.

In this work, for a 1:1 electrolyte solution with the concentrations c_{a}, c_{c} for cations and anions, respectively, and the

concentration c_p for ion pairs we will write eq 8 in the form

$$\log y'_c = b_{ca}c_a + b_{cp}c_p$$
$$\log y'_a = b_{ca}c_c + b_{cp}c_p$$
$$\log y'_p = b_{cp}(c_c + c_a) \quad (9)$$

where we set $b_{cp} = b_{ap}$ because we cannot distinguish between them. We also assumed $b_{cc} = b_{aa} = 0$ because generally it is a good approximation to neglect interactions between ions of like charge. Also, one might expect that interactions of ion pairs with each other would be smaller than interactions of ions with ion pairs, so we have set $b_{pp} = 0$.

In contrast to the MSA, which calculates an activity coefficient y_i in the 1 mol dm^{-3} standard state, the extended Debye−Hückel model calculates activity coefficients in the l mol kg^{-1} standard state γ_i. The correction from one to the other at the given solution pressure is

$$c_i = m_i/V^*$$
$$\ln y_i = \ln \gamma_i + \ln V^*/V^0 \quad (10)$$

where V^0 is the volume of 1 kg of pure solvent, and V^* is the volume of solution per kg of solvent.[28]

The extended Debye−Hückel equation of Oelkers and Helgeson[29] is given by

$$\log \gamma_\pm = \frac{A_\gamma z_i^2 \sqrt{I}}{1 + a^\circ B_\gamma \sqrt{I}} + \Gamma_\gamma + b_{\gamma MX} I$$
$$\log \gamma_p = \Gamma_\gamma + b_{\gamma MX^0} I \quad (11)$$

where I is the ionic strength in molality units, z_i is the charge on the ith species, a° denotes the ion size parameter, A_γ and B_γ represent the Debye−Hückel terms defined by

$$A_\gamma = \frac{1.8248 \times 10^6 \sqrt{\rho^0/1000}}{(\epsilon T)^{3/2}}$$
$$B_\gamma = \frac{50.291 \times 10^{10} \sqrt{\rho^0/1000}}{\sqrt{\epsilon T}} \quad (12)$$

where ρ^0 is the water density (kg m^{-3}) and Γ_γ denotes the mole fraction to molality conversion factor given by

$$\Gamma_\gamma = -\log(1 + 0.0180153 m^*) \quad (13)$$

with m^* standing for the sum of the molalities of all solute species in solution.

In their use of this equation, Oelkers and Helgeson[30] included only the ion−ion interactions ($b_{\gamma MX}$) and the effect of the ions on the activity of the pair ($b_{\gamma MX^0}$) but not the effect of the pair on the activity of the ions. This is thermodynamically inconsistent as these interactions must be identical.

The $b_{\gamma MX^0}$ values presented by Oelkers and Helgeson[30] are physically unrealistic because they require very long-range repulsive interactions between an ion and an ion pair. This kind of long-range interaction is unprecedented. We take, as an example, the NaCl salting out coefficient reported by Oelkers and Helgeson[30] at 823 K and 100 MPa, $b_{\gamma MX^0} = 2.2$ kg mol^{-1}. This is one of the higher values of $b_{\gamma MX^0}$ tabulated for NaCl by Oelkers and Helgeson.[30] At the same time, the values for $b_{\gamma MX^0}$ of NaBr and NaI under similar conditions are about twice as large, and the value for $b_{\gamma MX^0}$ of HBr is about 45 times larger at the same temperature and pressure.

Taking our model as that of hard spheres in a continuous dielectric medium, it is easy to calculate the second osmotic virial coefficients from the known ionic radii of the ions. This puts an upper limit on physically realistic values of b_{ij} for this model. It seems to us that this constraint also applies approximately to the real aqueous solution. A simple way of demonstrating the magnitude of the repulsive interactions required by $b_{\gamma MX^0} = 2.2$ kg mol^{-1} is to translate these salting out coefficients into forces at the molecular level. We assume that all of the repulsive interactions are concentrated in a hard core so that the two particles cannot approach each other closer than a hard core diameter, σ. We completely neglect the electrostatic forces that on average will be attractive (giving a negative $b_{\gamma MX^0}$). Using statistical mechanics, it is then easy to calculate the hard sphere diameter that would give this salting out coefficient, assuming there are no attractive interactions outside σ. The result of this calculation is that the ion cannot approach closer to the ion pair than about 13 Å. A rough calculation shows that physically realistic models must have b_{ij} approximately a factor of 10 smaller than this. It is also known that no such strong repulsive interactions are present in room temperature aqueous solutions. Friedman and co-workers[31−33] have shown that for alkali halides at room temperature the ions frequently penetrate to contact. One would expect that any repulsion caused by strongly hydrated water molecules around both the ion pair and the ion should be even lower at higher temperatures and lower densities because (1) the bulk density of the water is much less, making it easier for an ion to penetrate the hydration shell of the other ion; and (2) the dielectric constant of water is much lower, so the electrostatic forces attracting the ion to the pair are much larger. It is also hard to envision how such strong repulsive forces could be compatible with the triple-ion formation that is postulated by Oelkers and Helgeson.[1,29]

It should also be noted that Walther[34] in his discussion of the interaction parameters of neutral species in supercritical water concluded: "b_{ij} for neutral ion pairs most likely decrease with increasing temperature becoming negative in supercritical aqueous solutions".

Oelkers and Helgeson[30] derived these large values of $b_{\gamma MX^0}$ by fitting the empirical Shedlovsky equation[20] to the literature conductance data of 1:1 electrolyte solutions at $m \leq 0.1$ and ascribing all differences to a salting out coefficient. As will be shown below, when we use the more accurate equation of Turq et al.,[14] large salting out coefficients are no longer needed to explain the conductance data.

We consider that at the present time the TBBK conductance equation is the best one for concentrations above 0.01 mol dm^{-3}. It is worth mentioning that for dilute solutions (with concentration less than 0.01 mol dm^{-3}) the classical FHFP[35] conductance equation is more accurate, according to our experience and to Fernández-Prini and co-workers.[36]

3.4. TBBK Conductance Model. In the TBBK model, the Fuoss−Onsager continuity equations were solved directly by a Green's function technique with the MSA pair distribution functions for the unrestricted primitive model (different ionic sizes). The single electrolyte solution consists of two types of free ions with total conductance given by

$$\Lambda_F = \lambda_1^F + \lambda_2^F \quad (14)$$

where

$$\lambda_i^{\mathrm{F}} = \lambda_i^{\,0}\left(1 + \frac{\delta\nu_i^{\mathrm{el}}}{\nu_i^{\,0}}\right)\left(1 + \frac{\delta X}{X}\right) \tag{15}$$

is the ith ion conductance. In the last expression, λ_i^0 is the limiting equivalent conductance at infinite dilution, $\delta\nu_i^{\mathrm{el}}/\nu_i^0$ is the free ion electrophoretic velocity effect, and $\delta X/X$ is the free ion relaxation force correction. The ion velocity at infinite dilution in electric field E is defined by

$$\nu_i^{\,0} = e_i E\frac{D_i^{\,0}}{k_{\mathrm{B}}T} \tag{16}$$

where $e_i = z_i e$ is the electric charge of the ith ion, E is the electric field, and D_i^0 is the diffusion coefficient of the ith ion,

$$D_i^{\,0} = \frac{\lambda_i^{\,0}RT}{|z_i|F^2} \tag{17}$$

where F is the Faraday number.

The electrophoretic effect is divided in TBBK into the first- and the second-order contributions:

$$\frac{\delta\nu_i^{\mathrm{el}}}{\nu_i^{\,0}} = \frac{\delta\nu_{i1}^{\mathrm{el}}}{\nu_i^{\,0}} + \frac{\delta\nu_{i2}^{\mathrm{el}}}{\nu_i^{\,0}} \tag{18}$$

The relaxation effect is split into the three contributions

$$\frac{\delta X}{X} = \frac{\delta X_1^{\mathrm{rel}}}{X} + \frac{\delta X_2^{\mathrm{rel}}}{X} + \frac{\delta X_1^{\mathrm{hyd}}}{X} \tag{19}$$

In TBBK the influence of the possible difference in absolute ion mobility on conductance is defined by parameter κ_q

$$\kappa_q^{\,2} = \frac{e^2}{\epsilon\epsilon_0 k_{\mathrm{B}}T}\frac{\rho_i z_i^2 D_i^0 + \rho_j z_j^2 D_j^0}{D_i^0 + D_j^0} \tag{20}$$

In the case of 1:1 electrolyte, this parameter becomes equal to κ, which is the inverse Debye screening length, and it does not depend on individual ion mobility. Thus, in the case of a 1:1 electrolyte solution, the conductance depends on the sum of equivalent ion conductivities at infinite dilution but not on their difference. The viscosity in the TBBK model is constant and equal to the viscosity of solvent (water).

3.5. Mixture Model. Sharygin et al.[16] reviewed the literature on mixing rules and found many different recommendations of essentially the same rule although for different properties and with varying refinements: Reilly and Wood,[15] Miller,[37] and Anderko and Lencka.[38] The consensus equation is for a solution with a molar ionic strength I_c

$$\kappa[I_c] = N\sum_{M=I}^{N_c}\sum_{X=1}^{N_a} x_M x_X \Lambda_{MX}[I_c] \tag{21}$$

where $N = \sum c_{\mathrm{M}} z_{\mathrm{M}} = \sum c_{\mathrm{X}}|z_{\mathrm{X}}|$ is the equivalent concentration, the sums are over all positive species M and all negative species X with Λ_{MX} calculated at molar ionic strength $I_c = (\sum c_{\mathrm{M}} z_{\mathrm{M}}^2 + \sum c_x z_{\mathrm{X}}^2)/2$. The equivalent fractions of species in solution are given by $x_{\mathrm{M}} = c_{\mathrm{M}} z_{\mathrm{M}}/N$ and $x_{\mathrm{X}} = c_{\mathrm{X}}|z_{\mathrm{X}}|/N$.

3.6. Restricted Primitive Model. The restricted primitive model considers the solution to be made up of hard sphere ions in a continuous dielectric fluid. The thermodynamic properties of this model have been extensively studied. They are functions of only two dimensionless parameters: strength of interaction, β^*, and a range of interactions expressed as a reduced ion concentration, c^*:

$$\beta^* = \frac{e^2}{4\pi\epsilon_0\epsilon k_{\mathrm{B}}Ta}$$

$$c^* = 1000cN^{\mathrm{A}}a^3 \tag{22}$$

where $a = (\sigma_{11} + \sigma_{22})/2$ is the distance of closest approach, N^{A} is Avogadro's number, and c is the molar ion concentration. It is expected that in a rough way that the behavior of real aqueous solutions will also scale with these parameters and we will use β^* as a measure of the strength of the ion interactions.

At high values of reduced densities c^* and high β^* (20−50), an ionic fluid is dominated by ion clusters as in the models of Gillan[39] and Pitzer and Shreiber.[40] However, there are different definitions of ion clusters. In Gillan's[39] definition, two ions are "directly linked" if they are separated by a distance less than some chosen value R; two ions are "indirectly linked" if they are connected by a chain of "directly linked" ions. The group of ions is called a linked cluster if every particle in it is directly or indirectly linked to every other particle in the group. Another definition was adopted by Laria et al.:[41] a set of ions form a cluster if they are within a sphere of radius, R. This model is physically more appealing and gives predictions consistent with the present results (see discussion section below). However, it is clear from the theory that one can use various definitions of what one considers as pairs or multiion aggregates, or, one can assume there are no pairs or other aggregates. All of these approaches, if done correctly, must yield the same observable properties.[42,43] As an example of this, one can even successfully assume that aqueous NaCl is completely ion paired at all temperatures, pressures, and concentrations[44] and get a very useful theory. Thus, it is strictly mere semantics to argue that ion pairs or triplets exist or do not exist. However, from a practical point of view, in most cases one of these models is much simpler and to be preferred.

In the model of hard spheres in a continuous dielectric medium near its critical point, it has been found helpful to define pairs and triplets in calculating thermodynamic properties. Oelkers and Helgeson[1,2] have used the calculated association constants of Gillan[39] to make provisional estimates of the association constants in aqueous alkali halide solutions at high temperatures. At each temperature and pressure they found the hard sphere diameter that would reproduce the measured pair association constant in aqueous solutions. Then they made the reasonable assumption that the same hard sphere diameter could be used to calculate the association constant for all of the higher order aggregates. The results of these provisional estimates were that in high-temperature hydrothermal solutions multiion aggregates became important above about 0.1 mol kg^{-1}. Also, in some solutions, the concentration of free ions increased slightly at higher concentrations, indicating some redissociation.

3.7. Very High Concentrations. As several authors have pointed out, the limiting situation at high concentrations of a model that considers stepwise multi-ion association is a single macroscopic multi-ion aggregate. This aggregate is essentially a solvated fused salt that still conducts electricity quite well. Since the TBBK equation does not consider that multi-ion aggregates contribute to the conductance by transfers inside the aggregate or by transfers between aggregates (see Brouillette et al.[10] and Reger et al.[45] for examples), this equation is useless

TABLE 3: Ion Interaction Parameters in Aqueous Solutions: $\beta^*/\epsilon/\rho^0$ for the KCl Data

	P, MPa			
T/K	20	100	200	300
473	3.11/35.6/878	2.89/ 38.3/924	2.71/ 40.9/966	2.58/ 43./1001
573		3.64/ 25.1/823	3.27/ 28.0/885	3.04/ 30.1/930
673		4.93/ 15.8/693	4.03/ 19.3/792	3.61/21.5/852
773		7.49/ 9.05/528	5.08/ 13.3/691	4.32/15.7/771
873		11.86/ 5.1/374	6.49/ 9.3/590	5.18/11.6/691

under these conditions. Of course, if we had a better conductance theory based on a more accurate pair correlation function, which itself was accurate for very strongly interacting solutions, then this theory would not have to consider any association at all.

Valyashko[12] considered the experimental results for concentrated electrolyte solutions at high *T* and *P*, such as the temperature coefficient of electrolyte solubility, the temperature dependence of the molar volume of the solutions, the electrical conductivity and the spectrophotometric data for the temperature stability of Cu(II) complexes.[11,46] All these results demonstrate the existence of the transition region for electrolyte solutions. The hydrothermal solutions with concentrations above the transition region have properties similar to anhydrous salt melts. For 1:1 electrolyte solutions this transition region is about 7.5 $\pm$ 1 mol kg^{-1}.

This transition region is in reasonable agreement with the hypothesis that when the diameter of an aggregate is not much smaller than the average distance between aggregates, the solution is probably best treated as a solvated ionic melt. Thus, we would expect to prefer a solvated ionic melt model when the average distance between ions, if arrayed in a cubic lattice, $d_{av} = (2N^A c)^{-1/3}$, is close to the distance between two solvent separated ions. If we consider the solvent separated distance to be about $d_{ss} = (\sigma_a + \sigma_c + \sigma_w)/2$, then the transition point to a solvated ionic melt would occur near $c = 8.6$ mol dm^{-3} for NaCl and $c = 6.7$ mol dm^{-3} for KCl.

4. Conductance Data and Their Analysis

4.1. High-Temperature KCl Conductance Data. *4.1.1 Fits with only Pairwise Association (K_2 only models).* First, we will consider models in which only pairwise association occurs (K_2 only models) and as a consequence redissociation is important. The β^* parameter measuring the strength of ion interaction in solution, eq 22, was calculated with the distance of closest approach, $a = 3.19$ Å, equal to the sum of crystallographic radii of K^+ (1.33 Å) and Cl^- (1.86 Å). The values of this parameter with the dielectric constant and density of water[21,47] are collected in Table 3, which also shows the temperature and pressure range of the data analyzed. The viscosity of water was calculated according to Sengers and Watson.[48] The results of the fit of the KCl data in Table 3 using the MSA model and the crystallographic radii used for the ionic diameters is given in Tables 4−6. The average absolute deviation (Table 6) of the fit is no more than twice the reported accuracy of the experimental data (2%). The values of Λ^0 and logK_2 of KCl are in a good agreement with the literature values.[9,49] Thus, the application of the TBBK equation with MSA activity coefficients to hydrothermal solutions with concentrations up to 4.5 mol kg^{-1} leads to accurate values for Λ^0 and K_2 with no other adjustable parameters.

Table 7 shows our attempt to fit conductance data with additional variation in the size of the hard sphere ions by scaling all of the ionic radii by a constant, HSC,

$$\sigma_i^{\text{eff}} = \text{HSC}\sigma_i \tag{23}$$

There is only a very slight improvement of data fit, and the scaling constant is between 0.9 and 1.0 with 95% confidence limits of $\pm$0.3 to $\pm$1.0, so HSC is not significant at this confidence level. The fitting parameters logK_2 and Λ^0 do not change appreciably when HSC is used (see Tables 4, 5, and 7).

We chose four data sets at state points with high reduced inverse temperature β^* parameters to compare the fits by the DH and MSA models. These results are presented in Table 8 and in Figures 2a−d, which show the data fits by DH, MSA, and MSA with b_{cp} adjusted. We have used the $b_{\gamma NaCl}$ data of Oelkers and Helgeson[29] in calculations for KCl conductance results. The value of $b_{\gamma KCl}$ calculated by Pokrovskii and Helgeson[50] is very close to $b_{\gamma NaCl}$. It should be noted that the $a°$ ion size parameter in eq 11 was always equal to 4 Å.[50] Table 8 shows that when no adjustable parameters were used in the activity models, then MSA and DH activity models can fit the conductance data with about the same accuracy and with close to the estimated experimental accuracy (2%). When b_{cp} is adjusted in the MSA model or equivalently $b_{\gamma MX^0}$ is adjusted in the DH model, the fit is only marginally better and the added parameters are not significant at the 95% confidence level. The treatment of the KCl conductance data with the DH model yields salting out parameters $b_{\gamma MX^0}$ that are 1 order of magnitude lower than those found by Oelkers and Helgeson,[30] who fit the Shedlovsky equation to sodium halide conductance data. Pokrovskii and Helgeson[50] also obtained large values of $b_{\gamma KCl^0}$ at temperatures 373−598 K from KCl activity data in the range

TABLE 4: Limiting Equivalent Conductance (Λ^0/S cm^2 equiv^{-1}) of KCl for MSA Fit

	P, MPa			
T/K	20	100	200	300
473	750 (30)[a]	710 (30)	680 (30)	660 (30)
573		930 (40)	870 (30)	820 (20)
673		1120 (30)	1030 (30)	970 (30)
773		1140 (60)	1090 (40)	1030 (30)
873			1085 (50)	1050 (30)

[a] The 95% confidence limits of the last digit are given in parentheses.

TABLE 5: logK_2 for Reaction of Ion Pair Dissociation in KCl Solutions for MSA Fit

	P, MPa			
T/K	20	100	200	300
473	0.3 (4)[a]	0.2 (4)	0.1 (3)	0.0 (3)
573		−0.1 (3)	−0.1 (2)	−0.1 (2)
673		−0.8 (1)	−0.6 (2)	−0.4 (2)
773		−1.6 (2)	−0.9 (2)	−0.6 (2)
873			−1.4 (1)	−0.9 (1)

[a] The 95% confidence limits of the last digit are given in parentheses. Thus 0.3 (4) means 0.3 $\pm$ 0.4.

TABLE 6: Average Absolute Deviation (AAD) in % for K_2 Only Fit with MSA Activities

	P, MPa			
T/K	20	100	200	300
473	3.0	3.3	3.6	4.0
573		2.5	2.4	2.2
673		2.3	2.3	2.3
773		2.9	2.2	2.1
873			3.2	2.4

TABLE 7: Fitting of KCl Conductance Data by K_2 Only Models with MSA Activities and HSC Variation

	T/K							
	573				673			
P/MPa	Λ^0	log K_2	HSC	AAD, %	Λ^0	log K_2	HSC	AAD, %
100	930 (30) [a]	−0.06 (40)	0.9 (10)	2.7	1120 (40)	−0.9 (2)	0.9 (4)	2.0
200	870 (30)	−0.15 (25)	0.9 (6)	2.3	1030 (40)	−0.6 (2)	1.0 (4)	2.3
300	825 (30)	−0.09 (20)	0.9 (7)	2.0	970 (40)	−0.4 (2)	1.0 (5)	2.1
	773 K				873 K			
100	1140 (60)	−1.6 (2)	1.0 (4)	2.9				
200	1090 (40)	−0.9 (2)	1.0 (4)	2.2	1090 (50)	−1.4 (2)	0.9(3)	2.7
300	1030 (40)	−0.6 (2)	1.0 (4)	2.1	1030 (40)	−0.9 (2)	1.0 (4)	2.5

[a] The 95% confidence limits of the last digit are given in parentheses.

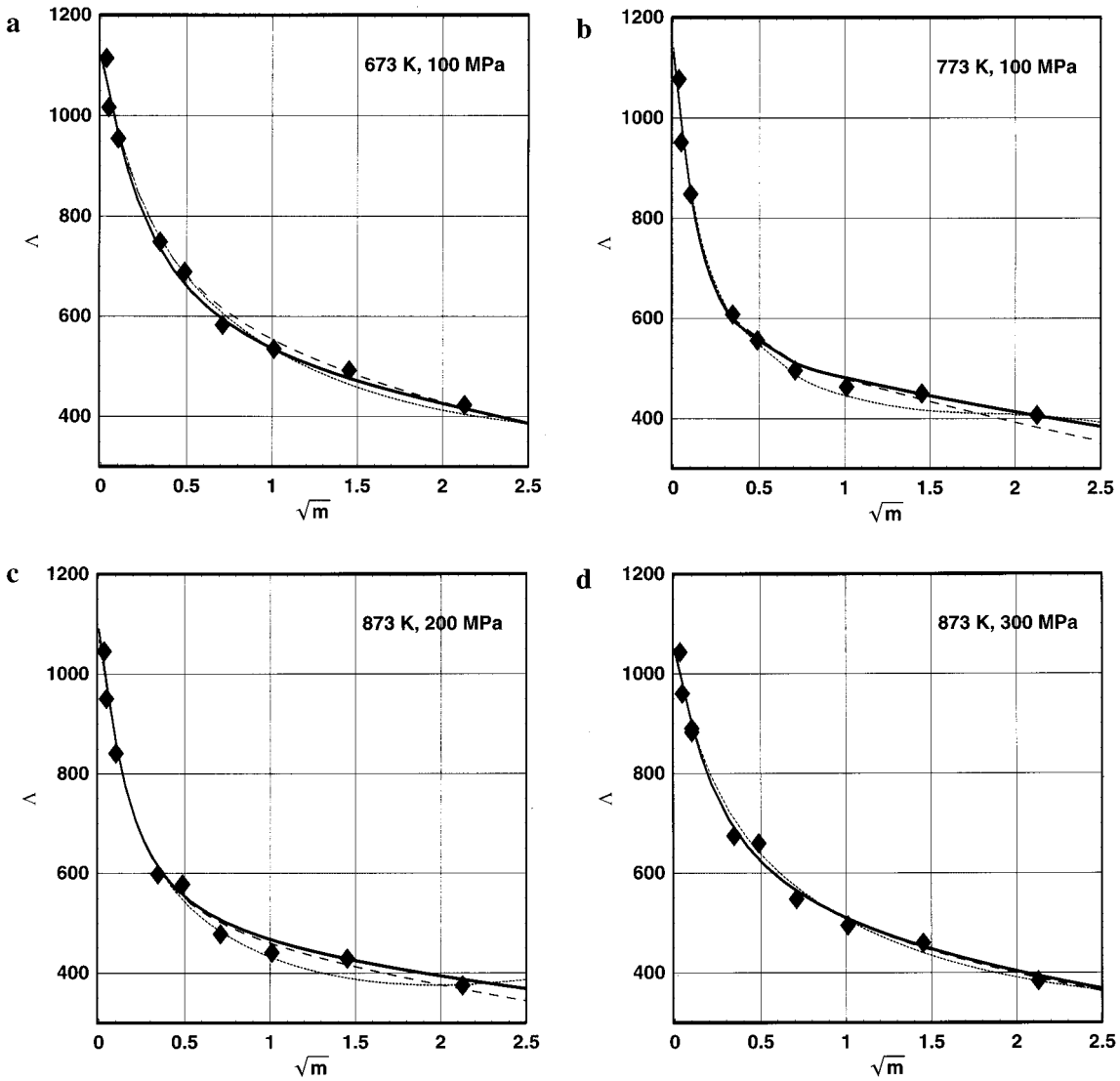

Figure 2. Fits of conductance data with K_2 only models: with MSA activity coefficients (dashed line), MSA with adjusted b_{cp} activity coefficients (solid line), and with DH activity coefficients (dotted line), models at four temperature and pressure points: (a) 673 K, 100 MPa; (b) 773 K, 100 MPa; (c) 873 K, 200 MPa; (d) 873 K, 300 MPa.

up to 6 mol kg^{-1}. Thus, a more accurate conductance equation does not confirm the values of $\beta_{\gamma MX^0}$ found by Oelkers and Helgeson.[30]

The concentration distributions of ions and ion pairs for the considered four data sets are shown in Figures 3a−d. These results indicate that the hydrothermal KCl solutions mostly consist of ions, the maximum fraction of ionpairs at 1 mol kg^{-1} is only about 30% (Figure 3), and redissociation can be extensive. As discussed above, the experimental accuracy is not sufficient to warrant additional adjustable parameters.

The MSA and extended DH models have activities with different concentration dependences. The mean stoichiometric activity coefficients of KCl for the two models on the molality scale are shown in Figure 4a. A clear difference between the MSA and extended DH models can be found for molalities above 2.25. The MSA model corresponds to the typical trend

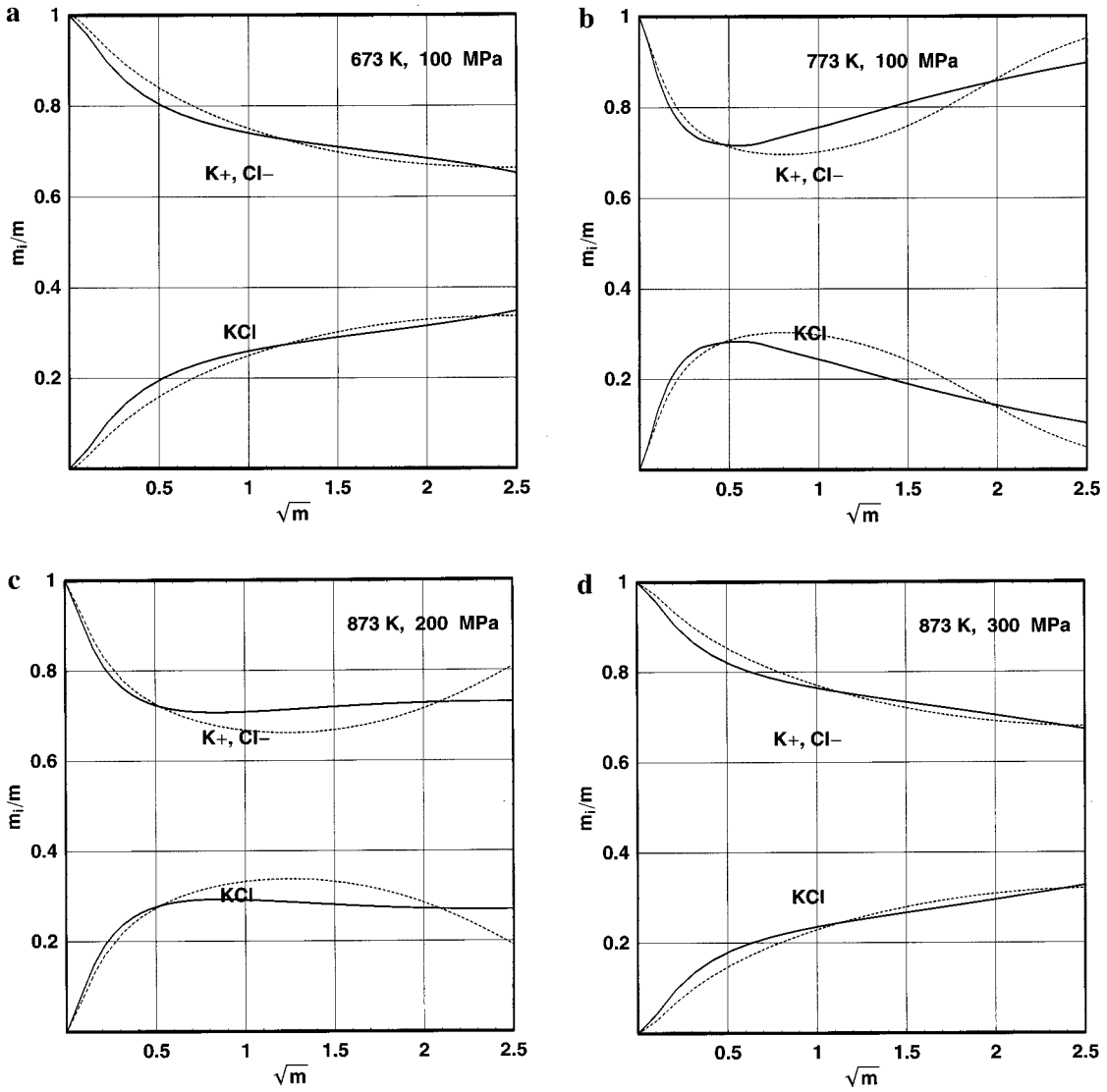

Figure 3. Concentration distribution of ions and ion pairs at four *TP* points corresponding to fitting by the TBBK conductance equation with K_2 only models. DH model (dotted lines) and MSA model (solid lines).

of KCl activity data. The results shown in Figure 4a can partially explain why the attempt to fit the DH model to activity data will produce a large $b_{\gamma KCl^0}$.[49] The two models give different ion activities starting from 0.25 mol kg^{-1}. In the MSA model, the anion and cation activities also differ starting from about the same molality (see Figure 4b). The ion activities are also low in magnitude compared to their concentrations.

4.1.2. Fits with Multi-ion Clusters. So far we have discussed fits with K_2 only models. We now consider multi-ion cluster models, in which clusters with more than two ions form. Our extensive calculations have shown that adding any appreciable amount of multi-ion cluster formation to either the MSA or DH activity models gives larger average errors to the fits because the calculated conductance is too low. This is illustrated in Figure 5 and Table 9, which show the poor results obtained by adding the provisional estimates of Oelkers and Helgeson[1] for K_3 and K_4 with $b_{\gamma MX^0} = 0$. However, if we adopt the values of $b_{\gamma MX^0}$ of Oelkers and Helgeson,[30] then we can fit the experimental results but we must add multi-ion cluster formation in order to fit the data, and the best values of K_3 and K_4 are not too far from the provisional estimates of Oelkers and Helgeson.[1] Table 10 shows the results of these fits. The high value of $b_{\gamma MX^0}$ raises the calculated conductance so that K_3 and K_4 are needed to lower it. Although this model fits the experimental conduc-

TABLE 8: Fitting of KCl Conductance Data to K_2 Only Models: Debye−Hückel and MSA Activities

Λ^0	log K_2	b_{cp}	model	$b_{\gamma MX}$	$b_{\gamma MX^0}$	AAD%
			673.15 K, 100 MPa			
1120(30)	−0.8(1)[a]		MSA			2.3
1120(40)	−0.9(2)	0.04(8)	MSA			2.0
1110(30)	−0.7(2)		DH	[−0.027][b]		2.5
1110(40)	−0.7(2)		DH	[−0.027]	0.05(9)	2.2
			773.15 K, 100 MPa			
1140(60)	−1.6(2)	-	MSA			2.9
1130(60)	−1.6(2)	0.06(12)	MSA			2.0
1120(50)	−1.5(2)		DH	[−0.115]		2.2
1110(50)	−1.5(2)		DH	[−0.115]	0.08(20)	1.8
			873.15 K, 200 MPa			
1085(50)	−1.4(1)		MSA			3.2
1090(50)	−1.4(2)	0.03(11)	MSA			2.7
1070(50)	−1.3(2)		DH	[−0.075]		3.4
1070(50)	−1.3(2)		DH	[−0.075]	0.01(10)	3.4
			873.15 K, 300 MPa			
1050(30)	−0.9(1)		MSA			2.4
1050(40)	−0.9(2)	0.01(15)	MSA			2.5
1040(40)	−0.7(2)		DH	[−0.022]		2.9
1045(40)	−0.8(2)		DH	[−0.022]	0.04(10)	2.8

[a] The 95% confidence limits of the last digit are given in parentheses. [b] The values in square brackets were taken from Oelkers and Helgeson (1990) (see text).

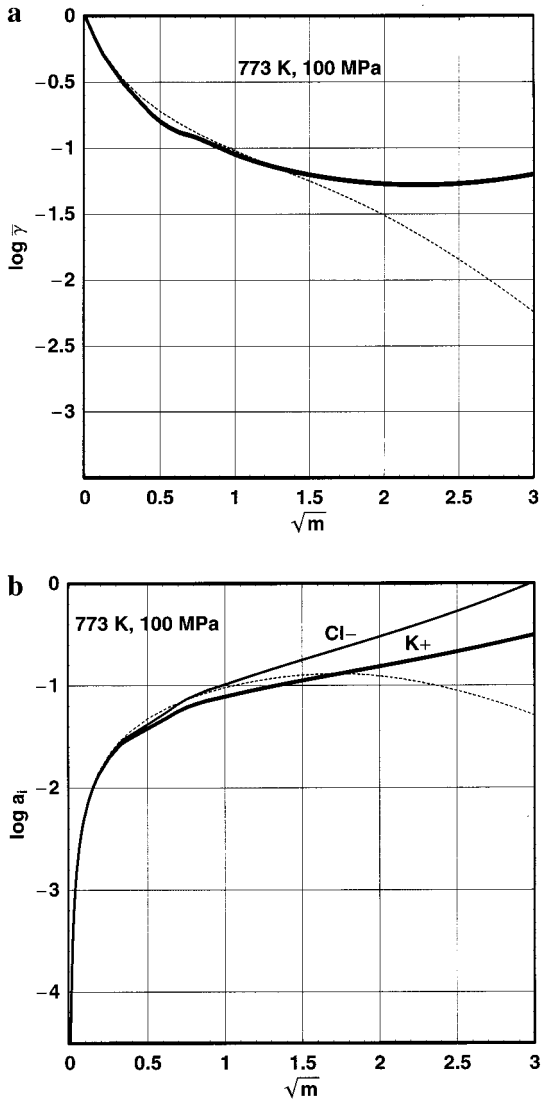

Figure 4. Concentration dependencies of activity relations in KCl electrolyte solution at 773 K and 100 MPa predicted by MSA (solid) and DH (dotted) models with K_2 only models. (a) Mean molal stoichiometric activity coefficient. (b) Free Cl^- and K^+ molal activities.

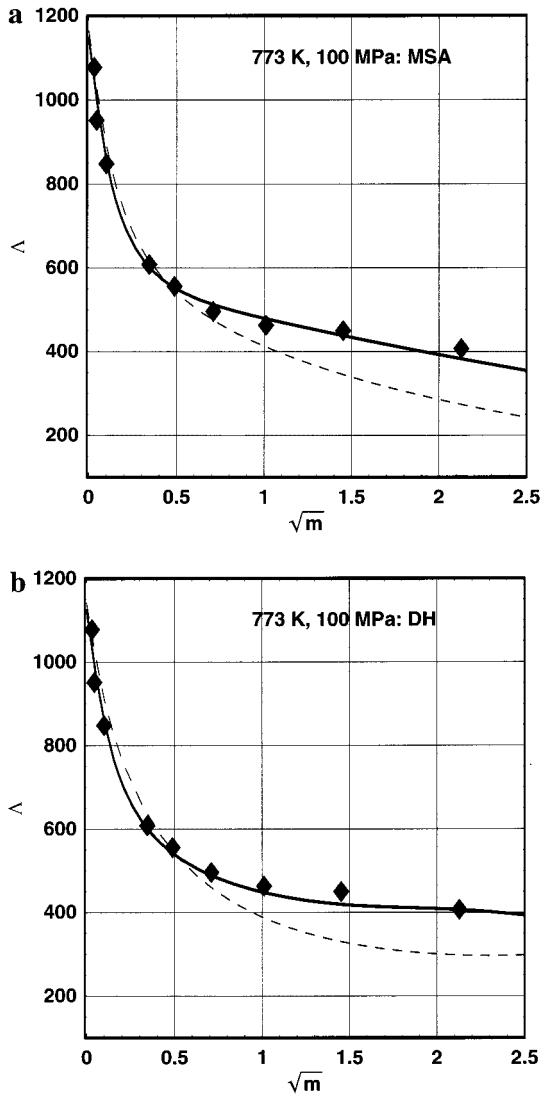

Figure 5. Different fits of (773 K and 100 MPa) KCl data by MSA (a) and DH (b) with $b_{\gamma MX^0} = 0$ models. The solid lines correspond to K_2 only models, see lines 1 and 3 of Table 8. The dashed lines show the fit with K_2 varying, K_3 and K_4 set to the provisional estimates of Oelkers and Helgeson, see Table 9.

tivities, we do not recommend it because it has two additional adjustable parameters (Occam's criterion) and it makes use of a salting-out coefficient that is both physically unrealistic (see section 3.3) and unnecessary to fit experimental data using the TBBK conductance equation.

4.2. NaCl Data at 651 and 670 K, 28 MPa. The distance of closest ion approach $a = 2.84$ Å was taken in correspondence with the crystallographic radius Na^+ (0.98 Å). The estimated experimental uncertainty of the NaCl conductance results is about 0.5%. The accuracy of the TBBK equation at concentrations above 0.5 mol kg^{-1} is unknown. The values of β^*, dielectric constant, and density of water are collected in Table 11. Table 12 gives the results of fits for NaCl at 651K with K_2 only models. The fit is reasonable (AAD = 1.6%) with only Λ_o and K_2 adjusted and with the MSA activity model. Adding an adjustable b_{cp} parameter in the MSA model is enough for achieving a fit close to the estimated experimental accuracy. The MSA, MSA+b_{cp} and DH fits are shown in Figure 6a. It is clear that adjusting the b_{cp} parameter results in an additional but not a large redissociation. In the investigated range of concentrations, the calculated activity data are essentially similar for the MSA and DH models (see Figure 6b). As with the KCl data, multi-ion cluster models do not improve the fits.

TABLE 9: Fitting of KCl Conductance Data (773K and 100 MPa) to Multiion Cluster Models

	log K_2	Λ_T^{0c}	log K_3	log K_4	Model	AAD, %
1160(170)	−1.5 (8)[a]	1000	[−1.6][b]	[−3.26]	MSA	9.8
1140(170)	−1.3 (12)	1000	[−1.6]	[−3.26]	DH	11.0

[a] The 95% confidence limits of the last digit are given in parentheses. [b] The values in square brackets were taken from Oelkers and Helgeson[1] (see text). [c] Λ_T^0 is the estimated equivalent conductance of the triplet ions (Na_2Cl^+ and $NaCl_2^-$).

At 670 K and 28 MPa, the ion interaction parameter is the highest of all the data, $\beta^* = 17.8$ (see Table 11) and these conditions are very close to the region where the solution exhibits phase separation. The results of fits to K_2 only models with the MSA and DH activity models are presented in Table 13 and Figure 7. These results show that without adjustable parameters the MSA and DH models deviate remarkably from the experimental results. The MSA model with two additional parameters, b_{ca} and HSC, is reasonable (ADD = 2.5%) but still not near the experimental accuracy of these data (~0.5%). Figure 7 shows that the adjusted values of Λ^0 and K_2 with either MSA or DH activities do not fit the data above about 0.05 mol

TABLE 10: Fitting of KCl Conductance Data to K_2 Only and Multiion Cluster Models: Debye−Hückel Activity Model with $b_{\gamma MX^0}$ as Suggested by Oelkers and Helgeson

Λ^0	log K_2	log K_3	log K_4	AAD, %
773.15 K, 100 MPa $b_{\gamma MX} = -0.115$, $b_{\gamma MX^0} = 1.20$, $\Lambda^0{}_T = 1000$				
1080(70)	−1.5(4)[a]			6.6
1120(80)	−1.5(5)	−1.0(8)	−3.7(6)	2.7
1180(90)	−1.7(3)	[−1.6][b]	[−3.26]	5.2
873.15 K, 200 MPa; $b_{\gamma MX} = -0.075$, $b\gamma_{MX^0} = 1.02$, $\Lambda_0{}^T = 1000$				
990(90)	−1.2(6)			8.8
1080(70)	−1.4(4)	−0.9(6)	−3.1(7)	2.6
1100(60)	−1.4(3)	[−1.24]	[−2.71]	4.1

[a] The 95% confidence limits of the last digit are given in parentheses. [b] The values in square brackets were taken from Oelkers and Helgeson[1] (see text).

TABLE 11: Ion Interaction Parameters in Aqueous Solutions for the NaCl Data

T/K (28 MPa)	$\beta^*/\epsilon/\rho^0$
651.3	8.35/10.8/524
670.2	17.8/4.9/298

TABLE 12: Fitting of NaCl Conductance Data at 651.3 K, 28 MPa to K_2 Only Models: Debye−Hückel and MSA Activity Models

Λ^0	log K_2	b_{cp}	model	$b_{\gamma MX}$	AAD, %
1250 (20)	−1.87 (5)[a]	-	MSA		1.6
1250 (10)	−1.90 (2)	0.4 (1)	MSA		0.5
1240 (50)	−1.8 (1)	-	DH	[−0.12][b]	3.9

[a] The 95% confidence limits of the last digit are given in parentheses. [b] The values in square brackets were taken from Oelkers and Helgeson[29] (see text).

TABLE 13: Fitting of NaCl Conductance Data at 670.2 K, 28 MPa to K_2 Only Models: Debye−Hückel and MSA Activity Models

Λ^0	log K_2	b_{ac}	HSC	model	$b_{\gamma MX}$	AAD, %
1200 (100)[a]	−3.6 (2)			MSA		26.7
1310 (20)	−3.57 (3)	1.0 (5)	1.5 (2)	MSA		2.5
1290 (70)	−3.62 (10)			DH	[−0.31][b]	9.4

[a] The 95% confidence limits of the last digit are given in parentheses. [b] The values in square brackets were taken from Oelkers and Helgeson[29] (see text).

kg^{-1}. At higher molalities, the experimental conductances are much lower, so either a positive b_{ca} (see Table 13, line 2) or substantial amounts of multiion clusters (see below) are needed to fit the data. The MSA and DH activity models lead to a high degree of redissociation at $m > 0.1$ mol kg^{-1}, which increases the conductance. This redissociaion is due to the rapid decrease of the ion activity coefficients, which in turn is due to the very high value of $\beta^* = 17.8$. At the same time, we should mention that at this high β^* parameter, the first and second order correction terms to the TBBK equation[14] no longer form a converging series at molalities above about 0.05 mol kg^{-1}. This circumstance increases the uncertainty in our calculations.

At this high value of β^*, the K_2 only models require additional parameters to achieve a reasonable fit to the data. A remarkable feature of this point is the fact that an accurate fit of the experimental data by a multi-ion cluster model is possible. The results for this model with MSA and DH activity coefficients are given in Table 14. Figure 8 compares the fits of experimental data at 670 K by both activity and multiion cluster models. The DH and MSA multiion cluster models with five adjustable parameters are equally good and fit the results with essentially the experimental accuracy (Table 14, lines 1 and 2). The fit of

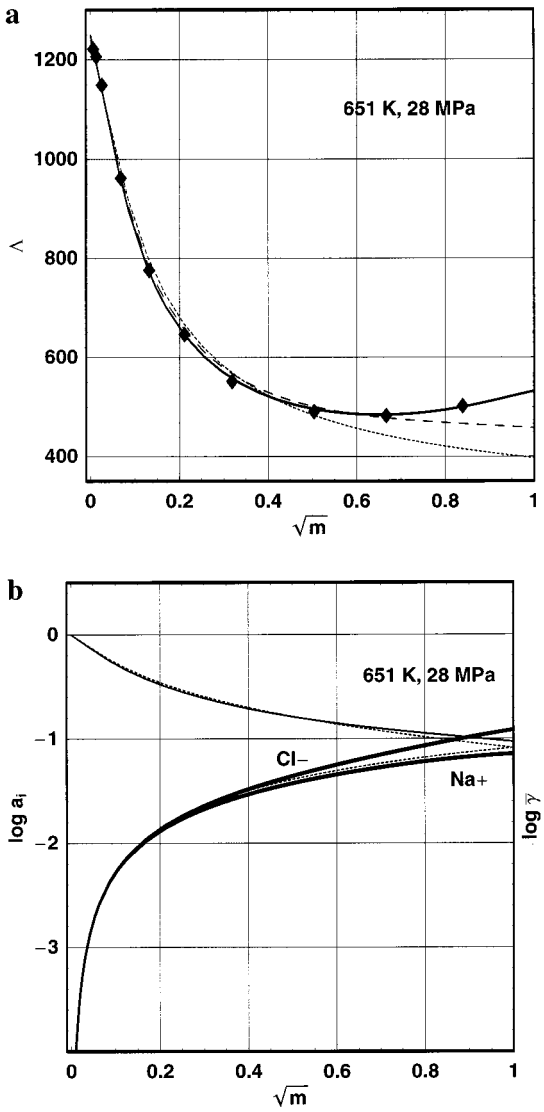

Figure 6. Fits of the NaCl conductance data at 651 K and 28 MPa. (a) K_2 only models with MSA (dashed line), MSA with b_{cp} varying (solid line), and DH (dotted line). (b) For the models in Figure 6a, Figure 6b gives the logarithm of the mean stoichiometric activity coefficient (upper lines) and activities of Na+ and Cl− ions on the molal concentration scale (lower lines). Dotted lines correspond to DH model with ion pairs; solid lines correspond to MSA model with ion pairs.

K_2 and Λ^0 with the MSA activity model with two adjustable parameters discussed above (Table 13, line 2) is also reasonable. It should be noted that the ion activities are lower in the case of the complex chemical model (see Figure 8b). The species distributions in solutions are very different for the two models (see Figures 9a and b). In the case of the model with K_2, K_3, K_4, and K_6, the maximum fractions of ion pairs, triple ions, and ion quadruples occur at molalities of 0.003, 0.5, and 0.1 mol kg^{-1}, respectively (Figure 9a). In contrast, the maximum fraction of ion pairs for the ion−ion interaction model is at 0.1 mol kg^{-1} (Figure 9b).

5. Summary and Discussion

It should be noted that in a recent paper Driesner et al.[51] reported an extensive study of the properties of the GROMOS models of Na^+, Cl^-, and SPC water. They found extensive multi-ion clustering in qualitative agreement with the predictions of Oelkers and Helgeson under conditions where we would need

TABLE 14: Fitting of NaCl Conductance Data at 670.2 K, 28 MPa to Multiion Cluster Models: Debye−Hückel and MSA Activity Models

Λ^0	log K_2	log K_3	log K_4	log K_6	model	$b_{\gamma MX}$	AAD, %
1310 (20)[a]	−3.56 (4)	−5.3 (1)	−8.7 (3)	−13 (1)	MSA	-	1.5
1315 (20)	−3.58 (4)	−4.2 (2)	−7.4 (10)	−11 (4)	DH	[−0.31][b]	1.5

[a] The 95% confidence limits of the last digit are given in parentheses. [b] The values in square brackets were taken from Oelkers and Helgeson[29] (see text).

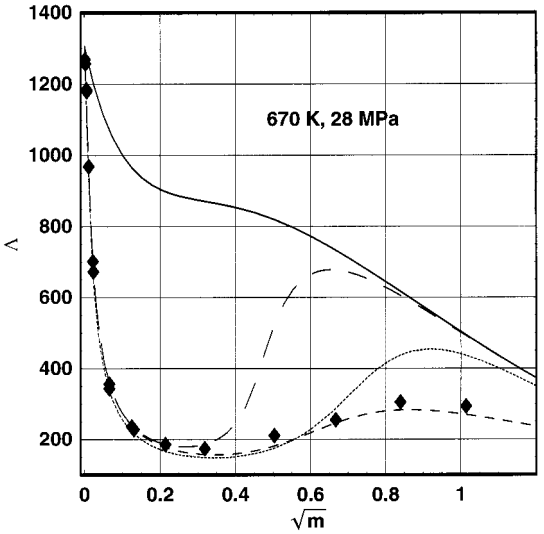

Figure 7. Least-squares fit of $NaCl_{(aq)}$ data at 670 K and 28 MPa. Solid line: fit with Λ^0 adjusted and no ion pairing and MSA activities. Long dashed line: fit with Λ^0 and K_2 adjusted and MSA activities (Table 12, line 1). Dotted line: fit with Λ^0 and K_2 adjusted with DH activities (Table 12, line 3). Short dashed line: fit with Λ^0, K_2, b_{ca} and HSC adjusted and MSA activities (Table 12, line 2).

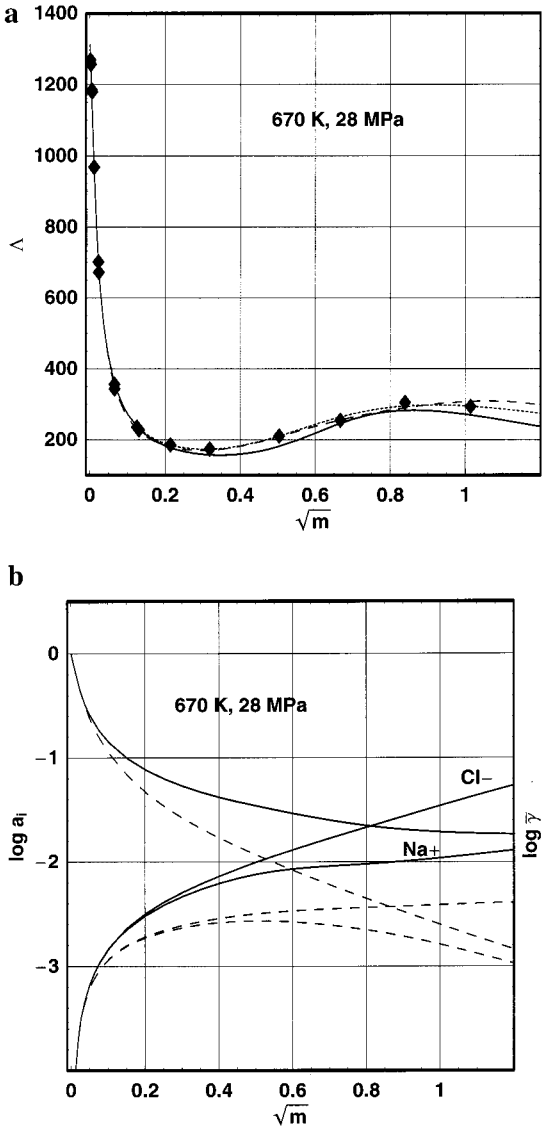

Figure 8. (a) Comparison of K_2 only and multi-ion cluster models at 670 K: DH with K_2, K_3, K_4 and adjusted (dotted line, see Table 13 line 2); MSA with K_2, K_3, K_4 and K_6 adjusted (dashed line); only model with MSA and b_{ca} activity coefficients and HSC adjusted (solid line). (b) Mean stoichiometrical activity coefficient and activities of Na+ and Cl− ions in molal concentration scale at 28 MPa and 670 K for the models in Figure 8a. Solid lines present MSA activity model with b_{ca} and HSC coefficients and ion pairs; dashed lines represent the MSA model with K_2, K_3, K_4 and K_6 adjusted.

only ion pairs to explain the conductance. However, Driesner et al. pointed out that their paper "should be considered as a reconnaissance study that provides the structural and dynamic information as a performance test of the intermolecular potentials at nonambient conditions". Thus the discrepancy with the present results may be due to inaccuracies in the GROMOS Lennard-Jones plus charge models. In a recent study Liu et al.[52] found that pairwise-additive, Lennard-Jones plus charge model could not represent accurate multibody ab initio ion + water potential energies.

Except for the one state point, at which the interactions are the strongest ($\beta^* = 17.8$), the simplest model that fits the experimental results reasonably well (±2−3%) at molalities up to 4.5 mol kg^{-1} is the K_2 only model with Λ^0 and K_2 adjusted. Activity coeficients calculated with either the MSA and ionic diameters or with the DH equation of Oelkers and Helgeson[29] (eq 11 with $b_{\gamma MX^0} = 0$) have similar accuracies. More complex models can also fit the data but they are not recommended. We take William Occam's point of view, "The mind should not multiply entities beyond necessity. What can be done with fewer... is done in vain with more."

For the state point with the highest β^* (NaCl at 670 K and 28 MPa), more complex models are needed at concentrations above 0.05 mol kg^{-1}. Good fits to the conductance results were found for multiion cluster models (five adjustable parameters and one assigned value for $\Lambda_o[MX_2^-]$) and reasonable fits were found with K_2 only models with complex activity models (four adjustable parameters), so that the models are about equally accurate at equal complexity for this solution.

It is interesting to note that in contrast to earlier cluster models,[40] the cluster model of Laria et al.[41] for the restricted primitive model is consistent with the qualitative predictions of our preferred simple activity model for aqueous solutions at high temperatures. For all values of β^*, complete redissociation is predicted in the model of Laria et al.[41] above 0.5 mol dm^{-3} because the optimum cluster radius goes below the hard sphere limit. They predict that appreciable amounts of multi-ion clusters are never formed when $\beta^* < 7$ and that pairs are more important than multi-ion clusters when $\beta^* < 14$, and this is consistent with our observations.

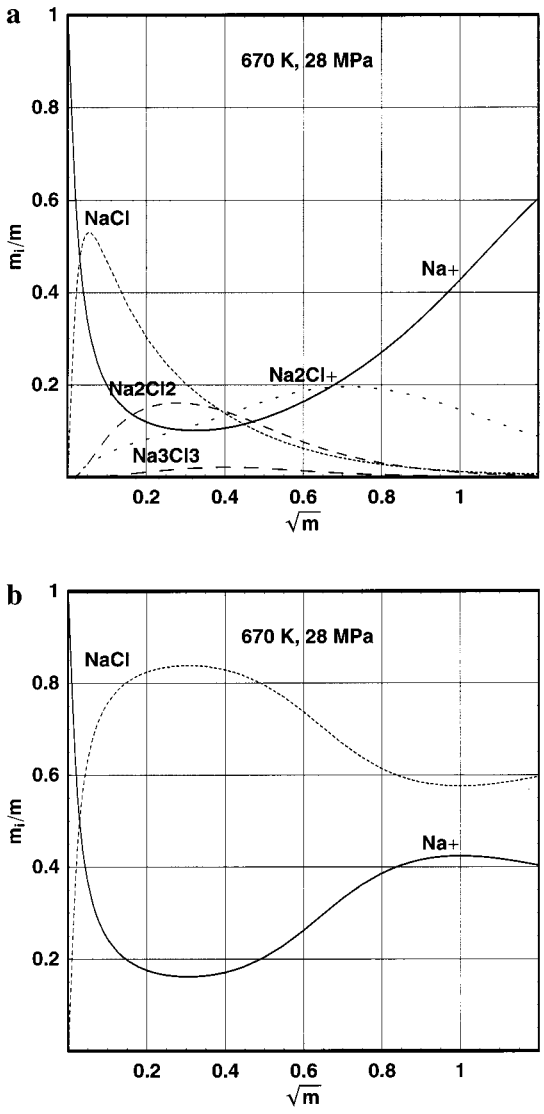

Figure 9. Molalities of various clusters divided by the stoichiometrical molality for NaCl at 670 K and 28 MPa. The $m[NaCl_2^-]$ (not shown) is very close but not equal to $m[Na_2Cl^+]$ since the activity coefficients are not exactly equal. (a) Complex chemical MSA model with polyatomic clusters. (b) K_2 only model with MSA and b_{ca} + HSC coefficients.

Acknowledgment. This research was supported by the National Science Foundation under grant number CHE9725163 and by the Department of Energy under grant number DEFG01-89ER-14080. The manuscript benefited from the anonymous reviewers. The authors thank Merik Gruszkiewicz, Eric Astle, and Marek Obsil for their help with the design and testing of earlier versions of the conductance apparatus. A suggestion by Eric Oelkers was one of the motivating factors for this research. Thanks go to Douglas Brunner for the diagram of the conductance cell and to George Rutynowski and the Department of Chemistry and Biochemistry machine shop for fabricating the apparatus.

References and Notes

(1) Oelkers, E. H.; Helgeson, H. C. *Geochim. Cosmochim. Acta* **1993a**, *57*, 2673−2697.
(2) Oelkers, E. H.; Helgeson, H. C. *Science* **1993b**, *261*, 888−891.
(3) Balashov, V. N. *Fluids in the Crust*; Shmulovich, K. I., Yardley, B. W. D., Gonchar, G. G., Eds.; Chapman & Hall: New York, 1995; 215−251.
(4) Noyes, A. A. *The electrical conductivity of aqueous solutions*. Carnegie Institution of Washington: Washington, DC, 1907; publication no. 63.
(5) Fogo, J. K.; Benson, S. W.; Copeland, C. S. *J. Chem. Phys.* **1954**, *22*, 212−216.
(6) Ritzert, G.; Franck, E. U. *Ber. Bunsen-Ges. physik. Chem.* **1968**, *72*, 798−808.
(7) Mangold, K.; Franck, E. U. *Ber. Bunsen-Ges. Phys. Chem.* **1969**, *73*, 21−27.
(8) Quist, A. S.; Marshall, W. L. *J. Phys. Chem.* **1968**, *72*, 684−703.
(9) Marshall, W. L. *J. Chem. Phys.* **1987**, *87*, 3639−3643.
(10) Brouillette, D.; Perron, G.; Desnoyers, J. E. *Electrochim. Acta* **1999**, *44*, 4721−4742.
(11) Hwang J. U.; Lüdemann, H. D.; Hartmann, D. *High Temp. High Pressures* **1970**, *2*, 651−669.
(12) Valyashko, V. M. *Ber. Bunsen-Ges. Phys. Chem.* **1977**, *81*, 388−396.
(13) Bernard, O.; Kunz, W.; Turq, P.; Blum, L. *J. Phys. Chem.* **1992**, *96*, 3833−3840.
(14) Turq, P.; Blum, L.; Bernard, O.; Kunz, W. *J. Phys. Chem.* **1995**, *99*, 822−827.
(15) Reilly, P. J.; Wood, R. H. *J. Phys. Chem.* **1969**, *73*, 4292−4297.
(16) Sharygin, A. V.; Mokbel, I.; Xiao, C.; Wood, R. H. *J. Phys. Chem. B* **2001**, *105*, 229−237.
(17) Zimmerman, G. H.; Gruszkiewcz, M. S.; Wood, R. H. *J. Phys. Chem.* **1995**, *99*, 11612−11625.
(18) Gruszkiewicz, M. S.; Wood, R. H. *J. Phys. Chem. B* **1997**, *101*, 6549−6559.
(19) Fisher, F. H.; Fox, A. P. *J. Sol. Chem.* **1979**, *8*, 627−634.
(20) Justice, J. C. In *Comprehensive Treatise of Electrochemistry*; Conway, B. E., Bockris, J. O'M., Yeager, E., Eds.; Plenum Press: London, 1983; Vol. 5, Chapter 3, p 310.
(21) Hill, P. G. *J. Phys. Chem. Ref. Data* **1990**, *19*, 1233−1274.
(22) Millero, F. J.; Ward, G. K.; Chetirkin, P. V. *J. Acoust. Soc. Am.* **1977**, *61*, 1492−1498.
(23) Majer, V.; Hui, L.; Crovetto, R.; Wood, R. H. *J. Chem. Thermodyn.* **1991**, *23*, 213−229.
(24) Vaslow, F. *J. Phys. Chem.* **1966**, *70*, 2286−2294.
(25) Friedman, H. L.; Dale, W. D. T. In *Modern theoretical chemistry. Vol.5, Statistical mechanics*; Berne, B. J., Ed.; Plenum Press: New York, 1977; Part A, p 85−135.
(26) Blum, L.; Høye, J. S. *J. Phys. Chem.* **1977**, *81*, 1311−1316.
(27) Chhih, A.; Turq, P.; Bernard, O.; Barthel, J. M. G.; Blum, L. *Ber. Bunsen-Ges. Phys. Chem.* **1994**, *98*, 1516−1525.
(28) Robinson, R. A.; Stokes, R. H. *Electrolyte Solutions*; Butterworth Scientific: London, 1959.
(29) Oelkers, E. H.; Helgeson, H. C. *Geochim. Cosmochim. Acta* **1990**, *54*, 727−738.
(30) Oelkers, E. H.; Helgeson, H. C. *Geochim. Cosmochim. Acta* **1991**, *55*, 1235−1251.
(31) Rasaiah, J. C.; Friedman, H. L. *J. Phys. Chem.* **1968**, *72*, 3352−3353.
(32) Ramanathan, P. S.; Friedman, H. L. *J. Chem. Phys.* **1971**, *54*, 1086−1099.
(33) Friedman, H. L.; Krishnan, C. V. *Ann. N. Y. Acad. Sci.* **1973**, *204*, 79−99.
(34) Walther, J. V. *Geochim. Cosmochim. Acta* **1997**, *61*, 3311−3318.
(35) Fernández-Prini, R. *Trans. Faraday Soc.* **1969**, *65*, 3311−3313.
(36) Bianchi, H. L.; Dujovne, I.; Fernández-Prini, R. *J. Sol. Chem.* **2000**, *29*, *No.3*, 237−253.
(37) Miller, D. G. *J. Phys. Chem.* **1996**, *100*, 1220−1226.
(38) Anderko, A.; Lencka, M. M. *Ind. Eng. Chem. Res.* **1997**, *36*, 1932−1943.
(39) Gillan, M. J. *Mol. Phys.* **1983**, *49*, 421−442.
(40) Pitzer, K. S.; Schreiber, D. R. *Mol. Phys.* **1987**, *60*, 1067−1078.
(41) Laria, D.; Corti, H. R.; Fernandez-Prini, R. *J. Chem. Soc., Faraday Trans.* **1990**, *86*, 1051−1056.
(42) Guggenheim, E. A. *Trans. Faraday Soc.* **1960**, *56*, 1159−1164.
(43) Petrucci, S.; Eyring, E. M. *J. Phys. Chem.* **1991**, *95*, 1731−1736.
(44) Stillinger, F. H.; Lovett, R. *J. Chem. Phys.* **1968**, *49*, 1991−1994.
(45) Reger, A.; Peled, E.; Gileadi, E. *J. Phys. Chem.* **1979**, *83*, 873−879.
(46) Scholtz, B.; Lüdemann, H. D.; Franck, E. U. *Ber. Bunsen-Ges. Phys. Chem.* **1972**, *76*, 406−409.
(47) Archer, D. G.; Wang, P. *J. Phys. Chem. Ref. Data.* **1990**, *19*, 371−411.
(48) Sengers, J. V.; Watson, J. T. R. *J. Phys. Chem. Ref. Data* **1986**, *15*, 1291−1314.
(49) Oelkers, E. H.; Helgeson, H. C. *J. Phys. Chem.* **1988**, *92*, 1631−1639.
(50) Pokrovskii, V. A.; Helgeson, H. C. *Geochim. Cosmochim. Acta* **1997**, *61*, 2175−2183.
(51) Driesner, T.; Seward, T. M.; Tironi, I. G. *Geochim. Cosmochim. Acta* **1998**, *62*, 3095−3107.
(52) Liu, W.; Sakane, S.; Wood, R. H.; Doren, D. J. *J. Phys. Chem. A* **2002**, *106*, 1409−1418.